Hybrid NVH modeling approach: How numerical and experimental methods complement each other

M. Wegerhoff[a], T. Kamper[a,1], H. Brücher[a], R. Sottek[a]

[a]HEAD acoustics GmbH, Ebertstraße 30a, 52134 Herzogenrath, Germany

Abstract

The ever-increasing demand for shorter development times and cost savings means that important design decisions must be made at an early stage of the development process. This goal of saving time and reducing costs leads to an increased use of virtual prototypes.

However, by combining the methods of simulation and testing, the idea of saving time and reducing costs can be extended even further. In addition, in some cases the accuracy of the results can be increased compared to the approach based solely on numerical models or experimental results. Depending on the task and the availability of data (to build virtual prototypes), methods (to model certain physical phenomena) and physical prototypes, the optimal approach must be chosen. In a connected world, where development processes are distributed across different companies, the availability of data and physical prototypes becomes even more critical: companies need to share product features to create system models, but may not want to share development knowledge or product design details.

In the proposed talk, a combined method of measurement and numerical simulation to predict and analyze the NVH properties of an e-bike is demonstrated. In this specific case, the electric drive unit of an e-bike that is already in series production is installed virtually in a numerical model of a new e-bike prototype. The excitation and structural dynamics of the electric drive unit are derived from experiment using the method of *in-situ* blocked forces. This kind of source description is known from the experimental transfer path analysis. In parallel, the numerical model of the e-bike prototype is built using a bottom-up method. The vibrations of the carbon frame induced by the virtually mounted electric drive unit are analyzed. The validity of the approach is shown using experimental data. The model presented can be used for further investigation of the airborne noise excited by the electric drive unit and radiated by the frame, which will be shown in following publications.

Keywords

e-bike, NVH, FEA, composites, vibration, acoustics

1 Introduction

Figure 1 displays how system knowledge can be achieved during different stages of the product development process using different methods: there are analytic methods, CAE-based methods, test-based methods, and hybrid methods. Hybrid methods consist of a combination of at least two models of the other domains, but typically a combination of CAE-based models and test-based models. Figure 1 gives an example of when these methods can be applied during the development process and how extensive the potentially achievable system knowledge is. Please keep in mind that this visualization is a highly simplified representation of a sample process. For a specific development process the details may differ (e.g., the potential of test-based methods in comparison to CAE-based methods).

---

[1]Corresponding author.
E-mail address: tim.kamper@head-acoustics.com (T. Kamper)

The total level of available theoretical system knowledge increases as the development proceeds due to decisions such as the definition of geometries, materials, connections of parts, connections to parts of suppliers, and so on.

Analytic methods can be applied immediately in the earliest stages of the development process, but the level of system knowledge that can be achieved is limited due to the high level of abstraction and simplification of the models used.

CAE methods are the next to follow as the development process proceeds. As design-mistakes tend to become more and more costly further into the development process, one should try to start development based on CAE as early as possible. The system knowledge that can be achieved with CAE methods is high even in early stages of the development process. However, in this schematic representation the maximum system knowledge achievable with CAE methods is outperformed by test-based methods when physical prototypes are available in the later stages of the development process. This can happen due to limitations in the accuracy of CAE-methods caused by hardware limitations, or the limitations of calculation methods for specific physical phenomena. However, this is not always the case. For simple structures or systems, it can also be vice versa.
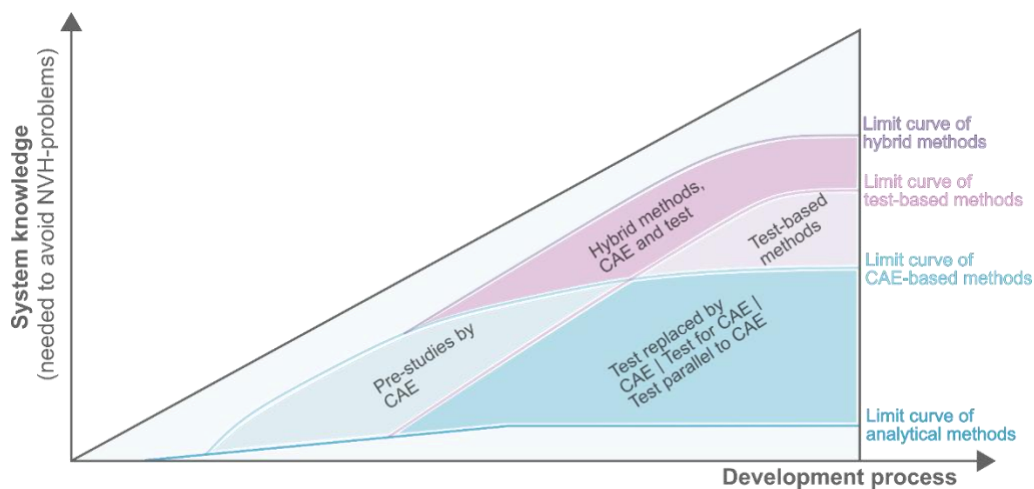

Figure 1. Advantages of combining test-based and CAE models for a development process that starts from scratch.

Finally, by the time physical prototypes of the components or the complete system are available, the test-based methods can be applied to gain more system knowledge. Besides the trend to make early design decisions possible based on CAE, there is a trend to reduce the number of necessary physical prototypes. Reducing the number of physical prototypes means replacing some of the test-based design decisions by CAE-based design decisions. Both trends are driven by the demand of shorter development times, cost reduction, and a large number of product variants.

This paper is about hybrid methods in the NVH domain, where numerical and test-based methods/models complement each other. Combining test-based and CAE-based methods results in more flexibility to pick the optimal method for a specific problem based on the available data, methods, computing power and physical prototypes. Hybrid methods have the potential to achieve a higher accuracy in results, generate more system knowledge and lead to better products [1].

The project discussed in this paper is divided into the steps displayed in Figure 2. In a first step, a measurement campaign is carried out with an e-bike of series production. With the method of *in-situ* blocked forces (see section 2.1) the drive unit is defined as an equivalent source of vibration. In the second step, a numerical model of an e-bike prototype is built to simulate the structural dynamics of the bicycle frame. The experimentally derived *in-situ* blocked forces from step one are used to excite the numerical model. To put it another way, you could say: The e-drive unit from series production is virtually installed into the prototype bicycle frame. As the output of the second step, the velocities on the surface of the frame are calculated. In the third step, a numerical model for calculating the sound radiation is set up, which takes the surface velocities calculated in the second step as input. In the fourth step, the predicted sound of the e-bike prototype is validated with a measurement campaign, and further analyses of the predicted sound are carried out using psychoacoustic parameters.

This paper covers the steps one and two. For more details on the steps three and four please see the following paper [1].
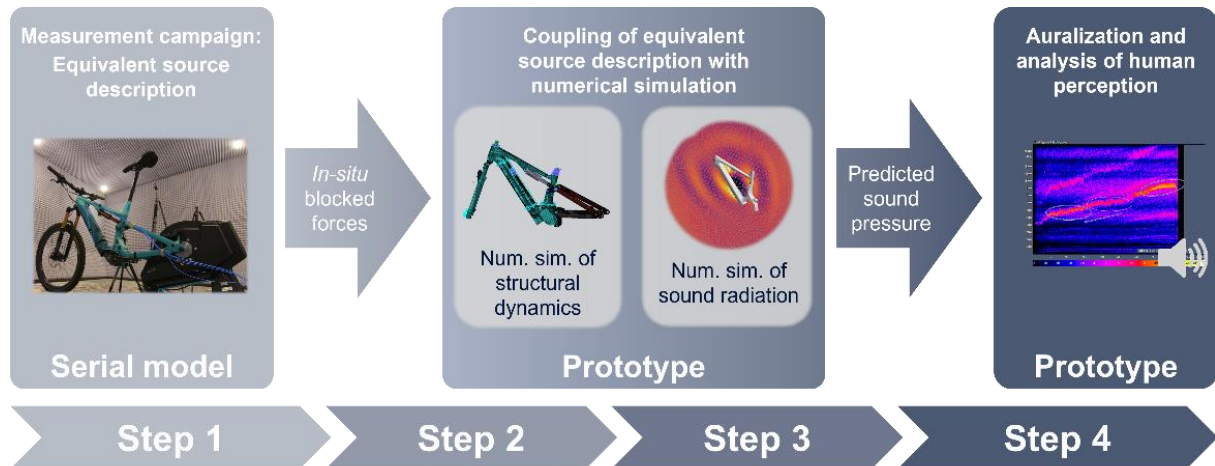
Figure 2. Flowchart of the entire process, the focus of this paper is on Step 1 and Step 2.

2 Application example

An electric-assist mountain bike was selected to demonstrate the capabilities of the hybrid NVH modeling approach. The e-bike consists of typical components such as drive unit, battery, frame, fork, rear swingarm, wheels, front and rear shock absorber.

Often the drive unit is a supplier part, and the drive unit is used in several e-bikes. For the evaluation of the acoustic properties of the e-bike, the drive unit must be coupled (virtually or physically) with the frame during the development process. However, in the early design phase, the frame of the e-bike might not be available as a real part, but only the drive unit from the supplier. If numerical models of the frame and the drive unit were available for the e-bike manufacturer, the drive unit and the frame could be virtually coupled and investigated as a system. However, normally the supplier does not provide a numerical model of the drive unit. The same applies to the data required by the e-bike manufacturer to create such a model of the drive unit on its own. In this situation, the hybrid modeling approach can support efforts to gain better insight into the acoustic behavior of the e-bike at an early stage of the development process. In the hybrid model, the excitation of the drive unit is represented by the experimentally derived *in-situ* blocked forces. These *in-situ* blocked forces can then be coupled with the e-bike frame, which is represented by a numerical model. For the determination of *in-situ* blocked forces the drive unit of interest is installed in any other e-bike with a similar mounting situation (previous e-bike generation, Step 1 in Figure 2). The measurement takes place on an e-bike test rig at HEAD acoustics. The derived *in-situ* blocked forces are transferred to the numerical model of the e-bike prototype (Step 2).

2.1 Concept and validation of an equivalent source description (in-situ blocked forces)

Several Transfer Path Analysis (TPA) methods are described in the literature. A comprehensive overview is given in [3]. The methods differ in the technical procedure and in the way of interpretation. In principle, by use of any of the documented methods it is possible to identify critical paths in a vibrating structure. A main difference between the methods is the definition of determined forces, which are used to describe the transfer paths between different subsystems. For transferring source descriptive forces from a test case to a simulation model, these forces need to be a property of the defined source exclusively rather than a property of the assembly (source and receiving structure). Therefore, Equivalent Forces (EFs), better known as *in-situ* blocked forces, are needed instead of directly measured operational forces, which are a property of both source and receiving structure. *In-situ* blocked forces can be determined indirectly via matrix inversion. Based on theory, no special test rig needs to be developed on which to mount the source. EFs are an interim result of the *in-situ* TPA. Any measurement for *in-situ* TPA is made on the coupled system; for example, a source mounted on a test rig, or a source coupled to a receiving structure. This is convenient and common for the experimental TPA and has the large advantage that the interface properties between the sub-structures are considered. In the following, the idea of the *in-situ* TPA is summarized. Elliott [4] addresses the *in-situ* approach as source characterization technique, done by measurements on the coupled structure.

Measured accelerations and Frequency Response Functions (FRFs) of the coupled system are used to determine EFs representing the source (see Figure 3). The index "op" stands for operational. The index "eq" stands for equivalent.
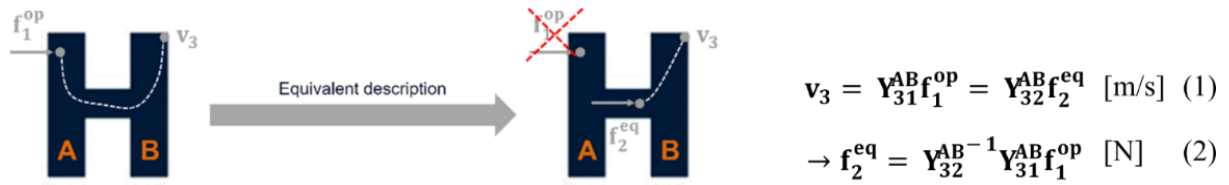

$$\mathbf{v_3} = \mathbf{Y_{31}^{AB}f_1^{op}} = \mathbf{Y_{32}^{AB}f_2^{eq}} \; [m/s] \;\; (1)$$

$$\rightarrow \mathbf{f_2^{eq}} = \mathbf{Y_{32}^{AB^{-1}}Y_{31}^{AB}f_1^{op}} \; [N] \;\;\; (2)$$

Figure 3. Idea of in-situ Transfer Path Analysis (TPA).

Based on velocities v and mobilities Y, the starting point for the description of $\mathbf{f_2^{eq}}$ is formulated in equation 1 in figure 3. The properties of $\mathbf{f_2^{eq}}$ need to be clarified to exploit the in-situ approach for the detection of a critical path. For equation 1 it is assumed that in addition to the original location of the excitation in point 1, any other location (e.g., point 2) can be defined at which a different type of force produces the same answer at point 3. This means that there is an equivalent description for the source, which no longer excites in point 1, but in point 2. The equivalent force in point 2 ($\mathbf{f_2^{eq}}$) is therefore different from the force in point 1 ($\mathbf{f_1^{op}}$) because of the influence of the structural dynamics of the structure under consideration, represented by the product of the mobilities ($\mathbf{Y_{32}^{AB^{-1}}Y_{31}^{AB}}$) in equation 2 in Figure 3.

2.1.1 Interface problem

For a valid source representation, it is essential that the determined EFs keep the source in position – ergo only a neglectable amount of energy is passing the interface between source and receiving structure. If this requirement is fulfilled, then the EFs are independent from the structural dynamics of the receiving structure; thus a transfer of EFs from the original assembly to a new assembly with modified receiving structure leads to valid results. Depending on the target frequency range and interface properties with respect to the coupled objects (assembly), the interface representation by EFs can become challenging. If the interface behaves like a rigid body, then one point with all translational and rotational degrees of freedom (DoFs) can represent the interface. However, if the interface behaves flexibly (which happens often above a few hundred Hz for drivetrain applications) then more points are needed. It is difficult to determine the required number of points. Too few points lead to an insufficient source representation (EFs are not valid), too many points lead to a high testing effort and large matrix size, which can imply an ill-conditioned matrix for matrix inversion. Therefore, the interface representation should be planned carefully. That is why a simple way of evaluating the planned/existing interface representation is needed. Simple means in best case, that with the needed data for *in-situ* TPA, the interface representation can also be judged. One possibility to evaluate the interface representation is the calculation of the Interface Completeness Criterion (ICC) published by Meggitt, Moorhouse and Elliot in [5], which is based mainly on data which are collected for *in-situ* TPA. Basic to the idea of the ICC is to take the measured transfer mobility from different excitation positions on the defined source to one receiver on the receiving structure and to compare them with the reconstructed transfer mobilities based on sub-structuring equations for the system with a chosen subset of interface DoFs. If the source is sufficiently represented, the original measured Transfer Mobilities from excitation points to Receiver (TMR) should be very close to the reconstructed TMR based on evaluation of sub-structuring equations. The advantage of ICC criterion is a good interpretability, as it provides a result between 0 and 1; an ICC of 1 implies a complete interface, whereas 0 indicates an incomplete interface. This idea was extended, called ICC+, and used in practical application. For further details see [6].

The interface between drive unit and e-bike is characterized by six screw connections (see Figure 4). Targeted frequency range is up to 1000 Hz. Due to the high stiffness of the drive unit and for space reasons, it was decided to represent each screw in the interface by a single point with three DoFs. In total, the interface is represented by 18 *in-situ* blocked forces.

In the following, the ICC+ evaluation will be discussed. As mentioned before, ICC+ only requires some additional excitations on the source side besides the measurements required for *in-situ* TPA. These excitations take place on the drive unit in y and z direction, since the first modes with participation of the interface are expected in these directions. For evaluation of the interface completeness, a receiver on the receiving structure needs to be defined (see Figure 4). The position on the lower tube is chosen because it is expected that the sound radiation is dominated by the lower tube. Therefore, the interface should be complete at least for the transfer path to the lower tube. Figure 5 shows the evaluation of the

ICC+. Based on the experience of the authors an ICC+ > 0.9 should be achieved. Up to 800 Hz this is the case. In the range of 500 Hz to 600 Hz the ICC+ just fulfills the requested value. Between 800 Hz and 950 Hz the interface definition does not seem to be complete. Above 1050 Hz the interface becomes increasingly incomplete.
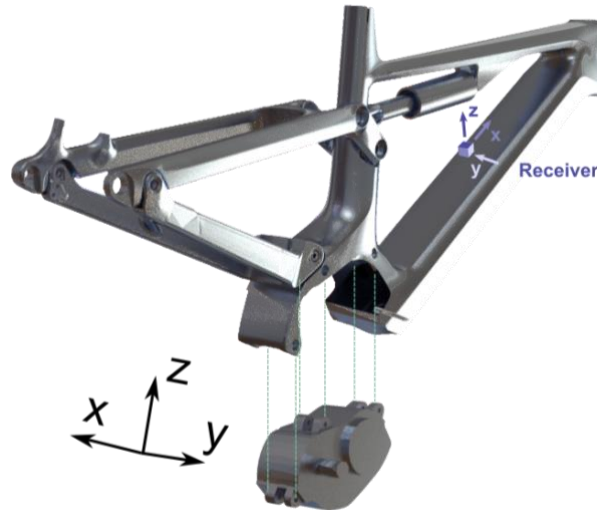

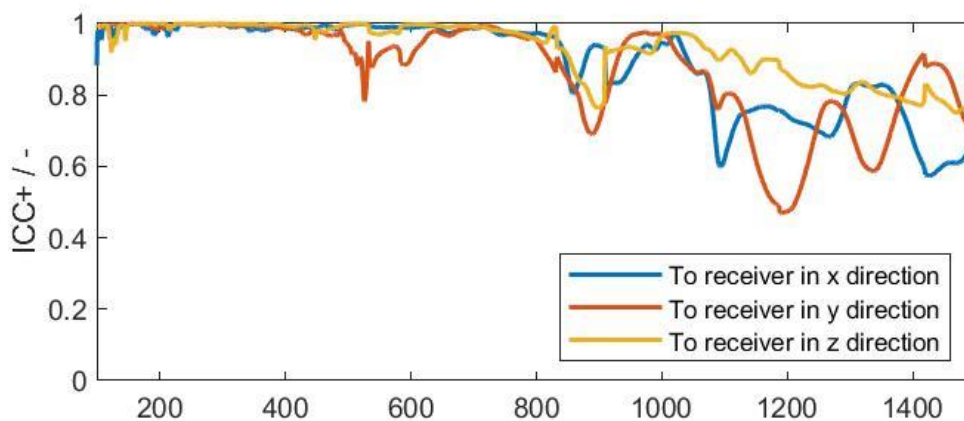Figure 4. Interface between drive unit and e-bike frame.

Figure 5. Interface completeness for the interface between drive unit and e-bike frame.

2.1.2 Validation of equivalent source (in-situ blocked forces) description

To gain valid results for the equivalent description, some analysis steps need to be done. Especially the interface between source and receiver needs to be properly defined [6]. As mentioned, the representation of the original system by *in-situ* blocked forces coupled with measured transfer functions should lead to the same result at the receiver position, in this case on the frame of the e-bike. For that a comparison is shown in Figure 6 for an acceleration output on the e-bike frame (receiver in Figure 4) versus time and frequency. For the frequency range of interest, good agreement can be found at this one point. At higher frequencies (>1050 Hz) differences between reference and resynthesis start to increase. Based on the examination of the ICC+ in the previous section, this is to be expected.

Anyway, one point on the structure-borne side is in general not quite convincing, that is why several output points [7], an integral output quantity (like airborne noise) or the comparison of forces are of greater interest.

For further validation in this work an additional measurement is carried out with an impact hammer as an artificial source on the drive unit. If the drive unit is rigid and accelerations are close to zero for the frequency range of interest, it is valid to compare the sum of all *in-situ* blocked forces in place with the original hammer excitation that occurred in the same direction (mechanical equilibrium). The result is shown in Figure 7. The y direction is transverse to the direction of bike travel (see Figure 4).
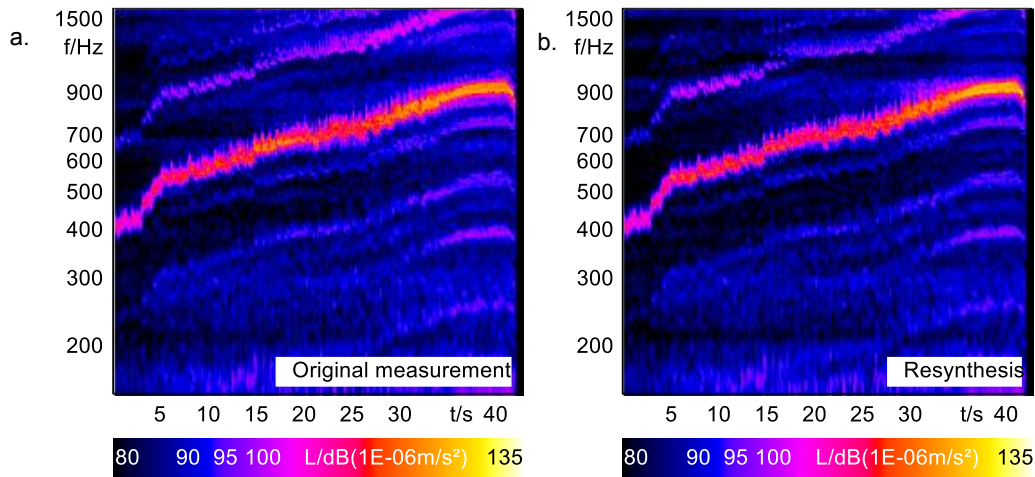
Figure 6.a. Comparison of accelerations for a run-up at a point normal to surface on the lower tube of the e-bike frame for original measurement, and b. for applied in-situ blocked forces on measured transfer functions, called resynthesis.
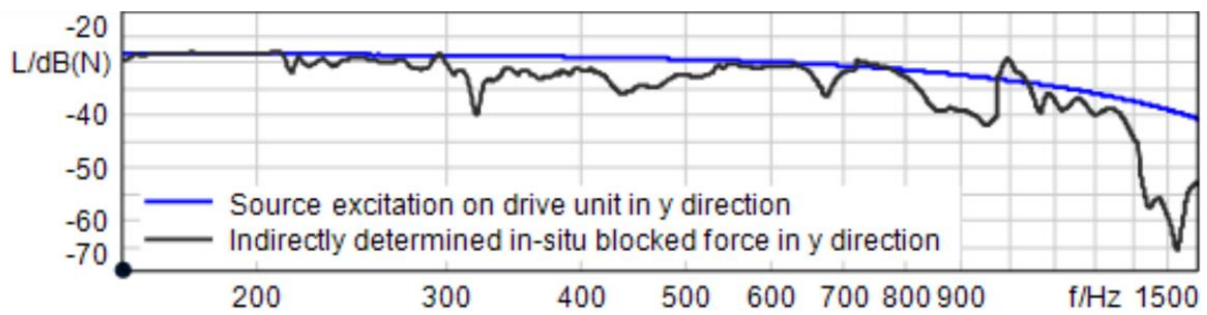

Figure 7. Comparison of forces for a hammer impact on drive unit between directly measured force (blue curve) and the sum of indirectly determined in-situ blocked forces about frequency.

The curves match very well considering the above-mentioned boundary conditions for the mechanical equilibrium, except in the range between 800 Hz and 950 Hz and above 1300 Hz. There can be several reasons for the mismatched areas: The drive unit is no longer rigid at such high frequencies (affects the mechanical equilibrium), or the defined interface for TPA is no longer complete or both. Based on the ICC+ evaluation an incomplete interface description is the best explanation. But based on the modeling of the numerical model it is also known that the drive unit becomes flexible starting at 750 Hz in free conditions. Therefore, there are overlaying effects that may be reasons for the deviations shown in figure 7 between 800 and 950 Hz.

2.1.3 Discussion of *in-situ* blocked forces

In total, the interface is represented by 18 *in-situ* blocked forces. The *in-situ* blocked forces are a property of structural dynamics of the drive unit and the excitation mechanisms within the drive (probably electromagnetic excitation, tooth meshing excitation, bearing excitation and general friction effects in contacts). Figure 8 shows the spectrum for each force. This is a peak hold FFT spectrum of a ~40 seconds run up. For the peak hold FFT spectrum not the quadratic mean value for each frequency is calculated, but instead the peak value from all calculated spectra is determined. The size of the time window is 0.17 seconds. The curves can essentially be divided into three frequency ranges. At lower frequencies, between 100 Hz and 400 Hz, general noise dominates the spectrum, probably caused by general friction inside the drive unit. Above 400 Hz, a dominant order appears, and as rpm increases, the excitation frequency naturally rises to 990 Hz at maximum rpm. The frequency range above 990 Hz is also characterized by excitation orders, but they are less prominent.
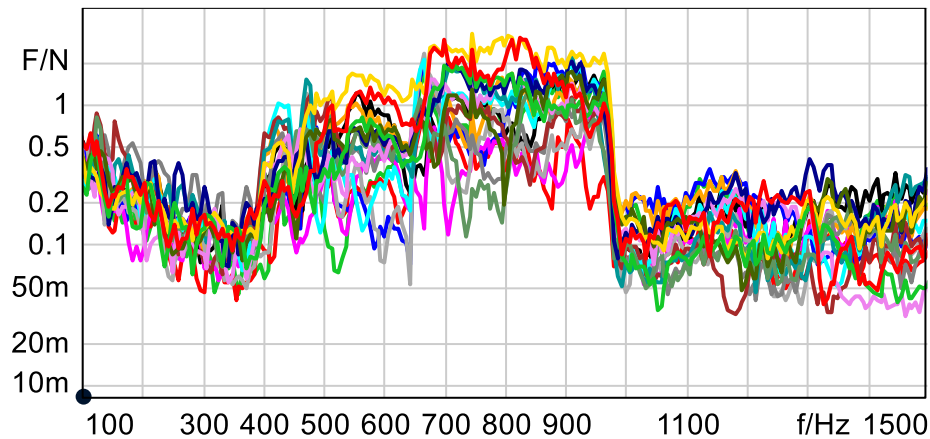
Figure 8. Peak hold frequency spectrum for the 18 in-situ blocked forces of the interface between drive unit and e-bike frame for a run up.

2.1.4 Summary of equivalent source description

For a wide frequency range of interest, the equivalent source description works very well. In the range of 800 Hz to 950 Hz the *in-situ* blocked forces representation shows weaknesses. Based on the validation the maximum error in this particular frequency range is estimated to be less than 10 dB. In Step 2, the *in-situ* blocked forces are applied to the numerical model.

2.2 Modeling of the structure-borne noise of the e-bike

Basically, the structure-borne noise consists of two components, one caused by excitation and the other by structural dynamics.

As mentioned earlier the determination of *in-situ* blocked forces as a property of excitation and structural dynamics of the drive unit is a known method in the context of test based *in-situ* TPA. In the test-based domain, the *in-situ* blocked forces must be paired with the receiver transfer functions of the assembled system. This means the *in-situ* blocked forces must be applied to a model in an *in-situ* configuration. For the hybrid method, a numerical model of the assembled system is chosen instead of measured transfer functions. Therefore, the numerical model consists of drive unit, battery, frame, fork, rear swingarm, front wheel, front and rear shock absorber.

For each component an appropriate modeling strategy needs to be chosen, considering the important physical phenomena to be represented by the model. In this case it is assumed that the e-bike frame dominates the acoustic radiation, especially the lower tube. That's why the frame needs to be modelled as a flexible part. It is assumed that the battery and the drive unit also affect the structural dynamics of the e-bike, but there are no data available for these components. Thus, modal analyses are performed as preliminary studies to determine the structural behavior of the respective components. At the mounting position of the rear wheel the e-bike is attached to the test rig. That is why this position is also assumed to be fixed in space in the numerical model. The front wheel, fork and shock absorber are represented just as mass and moment of inertia. The rear swing arm is modelled as flexible.

In order to apply different damping values to each component, the model consists of different substructures, where each substructure contains different modal damping values. The damping values are chosen based on empirical values or, if possible, taken from measurement. The complete numerical model is shown in Figure 9.

The final validation of the entire hybrid model is done in Step 4 based on the airborne signal [1]. However, some intermediate validation steps are useful and are also documented in this paper.
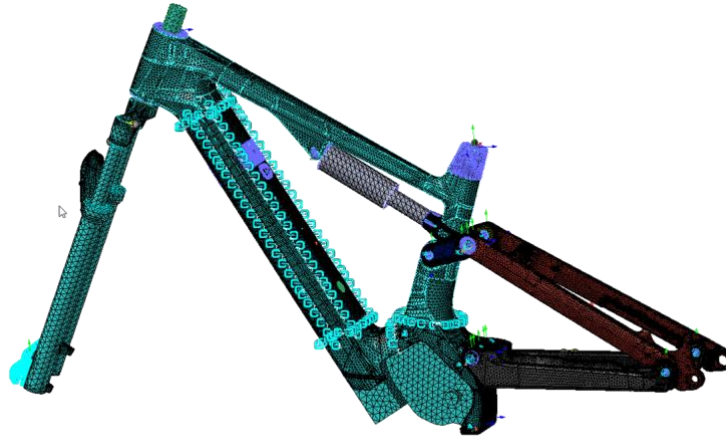
Figure 9. Overview about the finite element model of the e-bike.

2.2.1 Details about the frame model

The e-bike frame is made of Carbon Fiber-Reinforced Polymers (CFRP). For simulation the orientation of the layers and the anisotropic material properties must be known. Fortunately, some material prototypes were available for the estimation of the resulting material thickness. This was needed to adjust the configuration in the numerical model based on construction data.

During the project the frame itself was available at a later design stage so that a validation by an experimental modal analysis was done. In Table 1 an exemplary mode shape for the frame is shown.

Table 1. Example of shape comparison for the frame with focus on the lower tube.

Mode type	Test		Numerical simulation	
Mode with participation of lower tube	532 Hz		521 Hz	

2.2.2 Details about the battery and drive unit model
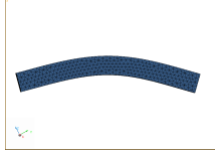
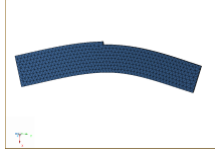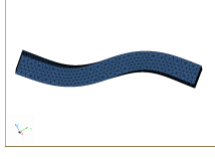The battery and drive unit are complex assemblies. In this project details about these components are unknown. That's why a detailed numerical model cannot be built up. Thanks to the physical availability of the components, models can be derived based on measurement data. For this purpose, an experimental modal analysis is done for the battery and for the drive unit. Resulting mode shapes and eigenfrequency values are used for a model updating of simple finite element structures of the battery and the drive unit.

In Table 2 the first bending modes of the battery are shown. These results are used for finding a Young's modulus for the finite element structure with the same outer dimensions as the real battery, and a determined density derived by weight measurement and known volume of the battery. Based on these input data the results of numerical simulation are displayed in Table 2.

The same procedure is done for the drive unit. However, the drive unit is much stiffer, which is beneficial for this approach since a numerical model can be kept simple. The first mode shape of the unmounted drive unit is about 750 Hz.

Table 2. First three measured and simulated bending modes of the battery.

Mode type		Test	Numerical simulation	
Longitudinal bending	100 Hz		103 Hz	
Transverse bending	150 Hz		149 Hz	
Longitudinal bending	234 Hz		268 Hz	

2.2.3 Application of *in-situ* blocked forces to the numerical model

As mentioned in the first chapter, the *in-situ* blocked forces for the drive unit, derived from a serial model e-bike, are applied to a new prototype e-bike. The *in-situ* blocked forces are in the time domain. The numerical simulation takes place in the frequency domain. Therefore, the time data need to be transferred to the frequency domain. Due to performance reasons, the data of the 40 seconds run-up is divided into 10-second sections with overlapping time windows at the beginning and ending of each section. For each section the structure-borne calculation is done and then passed to the airborne calculation in Step 3 [1]. At the end, in Step 4, the numerical simulation results are stitched together to reconstruct the entire run-up in time domain [1].

2.2.4 Discussion of exemplary output on prototype e-bike (receiver)

A detailed discussion of airborne results of the hybrid model is documented in [1]. In this paper an exemplary structure-borne output is shown to provide an insight about the interaction of drive unit and e-bike frame. Figure 10 shows a FFT vs. time analysis of a receiver position on the lower tube of the prototype frame, similar to the position on the serial model shown in Figure 4. The selected direction for the analysis is normal to the surface. The analysis reveals the excitation orders caused by the drive unit, represented by *in-situ* blocked forces. As described in the chapter "Discussion of *in-situ* blocked forces", one order in particular dominates the surface acceleration in the frequency range from 400 Hz to 990 Hz. Below 400 Hz, mostly noise is visible and at higher frequencies (>990 Hz) less-prominent orders appear.
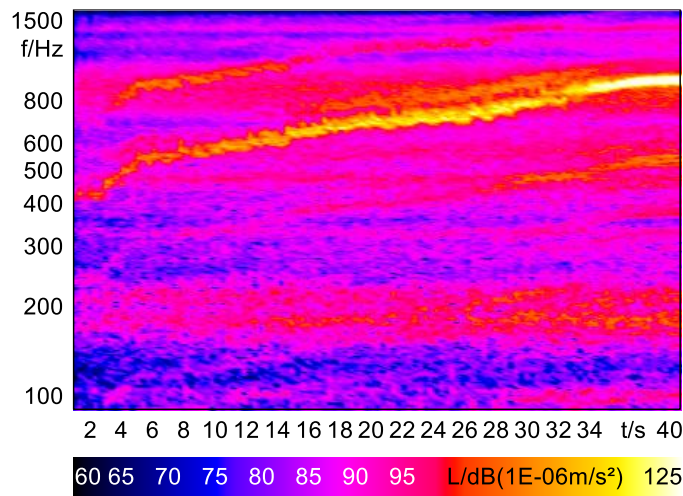

Figure 10. FFT vs. time for the acceleration sensor in simulation on the lower tube normal to the surface of the e-bike prototype.

3 Conclusions

This paper motivates hybrid modeling approaches and demonstrates the benefit of an approach using *in-situ* blocked forces with a real application example of high complexity. The study demonstrates how information gaps for the digitization of development processes can be overcome by combining test-based models and numerically-based models. Therefore, the approach offers an additional degree of freedom to meet the requirements for digital product development processes.

Intermediate validation steps serve to increase the reliability of the modeling approach. The final validation for airborne noise is performed and documented in [1]. Furthermore, the suitability of the airborne simulation results even for psychoacoustic analysis is demonstrated in [1].

In principle, this approach can be transferred to any other system where the separation between source and receiving structure is possible and where the subsystems can be assumed to be linear.

4 References

[1] M. Wegerhoff, B. Philippen, U. Ammerahl, and R. Sottek, "From simulation to auralization and human sound perception: A push button solution?" Keynote speech, Le Mans, Oct. 2021.

[2] T. Kamper, M. Wegerhoff, H. Brücher and R. Sottek, "Hybrid NVH modeling approach: High quality of NVH results enables psychoacoustic analysis of numerical computations," *Engineering Modelling, Analysis and Simulation*, vol. 1, Jan. 2024.

[3] M. V. van der Seijs, D. de Klerk, and D. J. Rixen, "General framework for transfer path analysis: History, theory and classification of techniques," *Mechanical Systems and Signal Processing*, vol. 68–69, pp. 217–244, Feb. 2016, doi: https://doi.org/10.1016/j.ymssp.2015.08.004.

[4] A. Elliott and A. T. Moorhouse, "Characterisation of structure borne sound sources from measurement in-situ," The Journal of the Acoustical Society of America, vol. 123, no. 5, pp. 3176–3176, May 2008, doi: 10.1121/1.2933261.

[5] J. W. R. Meggitt, A. T. Moorhouse, and A. S. Elliott, "On the Problem of Describing the Coupling Interface Between Sub-structures: An Experimental Test for 'Completeness,'" *Dynamics of Coupled Structures, Volume 4*, pp. 171–182, 2018, doi: https://doi.org/10.1007/978-3-319-74654-8_14.

[6] M. Wegerhoff, R. Sottek, and H. Brücher, "A Bridging Technology to Combine Test and Simulation with *In-Situ* TPA," *SAE Technical Paper Series*, Sep. 2020, doi: 10.4271/2020-01-1574.

[7] M. Wegerhoff, G. Jacobs, and P. Drichel, "Noise, vibration and harshness validation methodology for complex elastic multibody simulation models: With application to an electrified drive train," *Journal of Vibration and Control*, vol. 25, no. 2, pp. 243–254, Sep. 2018, doi: 10.1177/1077546318800124.